The anisotropy of the threshold energy for atom displacements in silver

1991 J. Phys.: Condens. Matter 3 3921

(http://iopscience.iop.org/0953-8984/3/22/004)

J. Phys.: Condens. Matter 3 (1991) 3921–3928. Printed in the UK

The anisotropy of the threshold energy for atom displacements in silver

W Sigle

Max-Planck-Institut für Metallforschung, Institut für Physik, Heisenbergstrasse 1, D-7000 Stuttgart 80, Federal Republic of Germany

Received 5 November 1990

Abstract. Individual grains of polycrystalline silver have been electron-irradiated at 473 K in a high-voltage electron microscope. The growth behaviour of interstitial-type dislocation loops is used to determine the anisotropy of the threshold energy for atom displacement $E_d(\omega)$. Local minima of the threshold surface of 13–14 eV are found in the ⟨100⟩ and ⟨110⟩ directions. Apart from these minima a large area of low E_d ($\simeq$ 17–19 eV) is found around ⟨110⟩ and a smaller region around ⟨100⟩ (19–20 eV). $E_d^{\langle 111\rangle}$ is only slightly higher than $E_d^{\langle 100\rangle}$ and $E_d^{\langle 110\rangle}$. The anisotropy of the threshold surface of silver is much more similar to that of Cu than that of Au, in spite of the fact that the ratio of ionic radius to interatomic distance is similar in Ag and Au. This result is discussed in terms of the electronic structure of Ag and Au and its influence on the propagation of replacement collision sequences.

1. Introduction

An ideal way to obtain information on directional effects in single crystals exposed to irradiation is the determination of the anisotropy of the threshold energy for atom displacement, $E_d(\omega)$. The threshold energy is particularly low in the direction in which the irradiating particles can excite replacement collision sequences (RCSs). These RCSs may propagate at low-energy loss mainly along certain low-index crystallographic directions.

A review of the anisotropy of the threshold energy of FCC metals has been given by Hohenstein *et al* (1989). A correlation of the easy directions for displacement and the material parameters influencing the propagation of an RCS (ionic radius R_0, interatomic distance d_0) was found. At large values of the ratio $\alpha = R_0/d_0$ (Au) ⟨100⟩-RCSs are preferred whereas at low α (Al, Ni, Cu) ⟨110⟩-sequences predominate.

The α value of Ag is only slightly lower than that of Au (which is the largest among the FCC metals). Therefore a behaviour similar to that of Au might be expected. We shall see that this is not the case. We consider this as further evidence for the special role of Au in the field of radiation damage.

In the past no systematic determination of the threshold energy anisotropy of Ag was performed. Only a few experimental threshold energy data exist for Ag (see section 4). The present paper reports for the first time on the determination of the anisotropy of E_d in Ag. The growth of interstitial-type dislocation loops was used to determine E_d (cf Urban and Yoshida, 1981). This technique is practicable at high temperatures where both vacancies and interstitial atoms are thermally mobile. Thus,

0953-8984/91/223921+08$03.50

apart from the information on the anisotropy, the threshold energy data obtained are of considerable technological interest.

The experiments were carried out in the high-voltage electron microscope (HVEM) of the Max-Planck-Institut für Metallforschung (AEI-EM7). The use of thin specimens is a prerequisite for the determination of the anisotropy of E_d. This is because multiple electron scattering weakens the dependence of radiation damage on the crystallographic direction. Furthermore, since the specimen orientation and the electron kinetic energy can be varied easily, the determination of the E_d anisotropy by electron microscopy is superior to other techniques used in this field.

2. Experimental procedures

Silver of 6N nominal purity was cold-rolled to a thickness of 0.1 mm. Specimens 3 mm in diameter and disc-shaped were punched out and subsequently recrystallized at 1170 K for 2 h. The polycrystalline samples were jet-electropolished at ambient temperature until perforation. A solution of glacial acetic acid, thiourea, methanol and sulphuric acid (Lyles *et al* 1978) was used. Irradiations were performed in the HVEM on individual grains, whose orientation with respect to the electron beam was adjusted with an accuracy of $\pm 1°$ using Kikuchi patterns. The electron energies used were 0.5, 0.6, 0.7, 0.8 and 1 MeV. The electron current density was 5×10^{23} e^- m^{-2} s^{-1}. Typical irradiation times were about 2000 s.

During all irradiations the specimen temperature was 473 K. Polished specimens were kept in a desiccator between the irradiations and were used for not more than 5 days. During such a period no change in the loop growth rate under identical irradiation conditions could be found. This presumably means that a thick oxide or sulphide layer did not grow on the specimen surface.

3. Experimental method

3.1. Growth and shape of dislocation loops

All dislocation loops were of the Frank type, presumably due to the very low stacking-fault energy of Ag. The low stacking-fault energy might also be the cause for the variety of loop shapes, although this is not yet understood. Whereas in metals with intermediate stacking-fault energies Frank loops grow in regular hexagonal shapes, in Ag triangular, trapezoid, parallelogram, rhombic and even more irregularly shaped loops were also observed. The dislocation lines were always straight ⟨110⟩ segments (figure 1).

The rate of interstitial absorption by a dislocation loop is proportional to the length of its circumference. Since the loop growth-rate was determined by measuring the temporal increment of a linear dimension of the loop (usually a diameter), the value obtained in this way depends on the loop shape. Therefore the loop growth-rates were normalized to the growth-rate of a regular hexagonal loop.

In some cases a correction was not possible. These were mainly loops elongated along a ⟨110⟩ direction and growing—mainly along this direction—at a much higher rate than all other loops. We suppose that such loops already nucleate in such an elongated shape and that the high sink efficiency of the long dislocation segments and the enhanced diffusion of interstitial atoms along the dislocation line is responsible for this phenomenon.

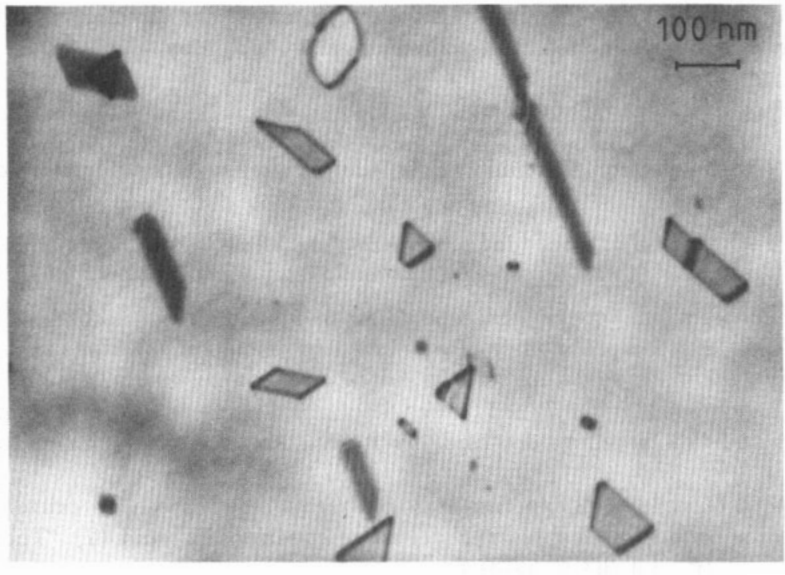

Figure 1. Dislocation loops as observed in Ag after electron irradiation at 473 K ($E = 600$ keV). The loop at the left edge has converted to a perfect loop with Burgers vector $(a/2)\langle 110\rangle$. Such loops as well as elongated loops like those in the top-left-hand corner were not used for the analysis. The elongated loops grow preferentially along the direction of elongation (cf section 3.1).

3.2. Determination of the threshold surface

At the irradiation temperature of 473 K both vacancies and interstitial atoms are mobile. Under such conditions dislocation loops grow linearly with the irradiation time, except for very small loops. In this case the dislocation line tension reduces the loop growth markedly. In order to avoid this complication the minimal diameter of the loops analysed was chosen to be 100 nm.

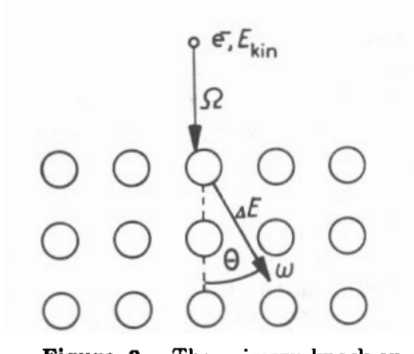

Figure 2. The primary knock-on of an electron (kinetic energy E, momentum direction Ω) onto a lattice atom. The lattice atom receives the energy ΔE and is displaced in the direction ω.

The loop growth rate v may be written as

$$v(E,\Omega) = CP^n(E,\Omega) \tag{1}$$

where E is the kinetic energy of the electron and Ω the direction of irradiation (see figure 2). The production rate of Frenkel pairs is given by

$$P(E,\Omega) = \sigma(E,\Omega)j. \tag{2}$$

Here j is the electron flux and $\sigma(E,\Omega)$ the total cross section for atom displacement:

$$\sigma(E,\Omega) = \int [\mathrm{d}\sigma(E,\omega)/\mathrm{d}\omega]_{\mathrm{Mott}} p(\Delta E, E_{\mathrm{d}}(\omega))\,\mathrm{d}\omega. \tag{3}$$

The term in square brackets denotes Mott's differential cross section and $p(\Delta E, E_{\mathrm{d}}(\omega))$ the probability of permanently displacing an atom that has received energy ΔE in a momentum transfer in the direction ω (figure 2).

The exponent $n = 0.72 \pm 0.06$ was determined by measuring v at different electron fluxes and the procedure described by Hohenstein *et al* (1989) gave $C = 40$ nm s^{-1} $(\mathrm{e}^-/\mathrm{s})^{-0.72}$.

With C and n the experimental total cross sections can be calculated from the measured loop growth rates $v(E,\Omega)$ using equations (1) and (2). These values are shown as full triangles in figure 5.

In order to deduce the threshold energy surface $E_{\mathrm{d}}(\omega)$† from these experimental data, the orientation triangle is divided in a number of segments (here 38) to each of which an E_{d} value is assigned. Equation (3) then yields theoretical values of the total cross section. Using a fitting procedure the 38 E_{d} values are varied such as to obtain a best fit to the experimental values.

The low-energy irradiations (here $E = 500$ and 600 keV) allow the determination of the position and E_{d} value of the minima in the threshold surface whereas the high-energy irradiations are necessary to determine the constant C.

4. Experimental results

The threshold surface obtained by the fitting procedure described in section 3 is shown in figure 3. The cross sections calculated with equation (3) (not shown in the figure) by using these data are in very good agreement with the experimental cross sections between 600 and 1000 keV. However, the E_{d} values of figure 3 are so high that the calculated cross sections for irradiations at 500 keV are zero which is contrary to the experimental data shown in figure 5. The reason for this unsatisfactory fit is that the area of the E_{d} elements is so large that a reduction in the E_{d} value which would improve the quality of the fit at 500 keV increases the cross sections at 600 to 1000 keV excessively. Since it is the 500 keV data which are most sensitive to the fine structure of minima of the threshold surface this discrepancy was improved by changing *fractions* of the E_{d} elements in such a way as to give a contribution to σ (500 keV). Since the maximal energy transferred to an Ag atom by a 500 keV electron is 15.1 eV, this can be achieved by reducing E_{d} of such fractions below 15.1 eV. The threshold surface obtained in this way is shown in figure 4. It must be emphasized that the degree of agreement between σ^{theo} and σ^{exp} at 500 keV is very sensitive to small changes in both the size and position of these local minima. This holds especially for the minima

† The term 'threshold energy surface' means the illustration of the threshold energy values in the orientation triangle.

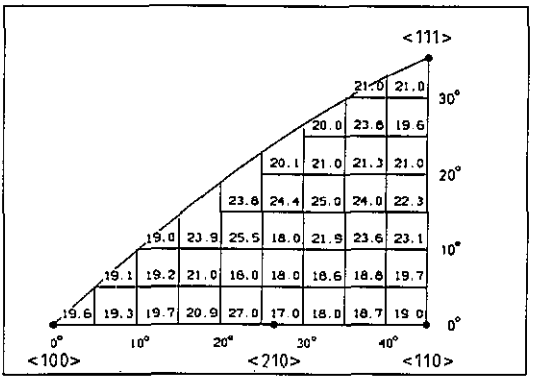

Figure 3. This figure shows the altered version of the threshold surface of figure 3. Small areas of threshold energies below 15.1 eV (= ΔE_{max} (500 keV)) were also inserted in order to give a good reproduction of the 500 keV data.

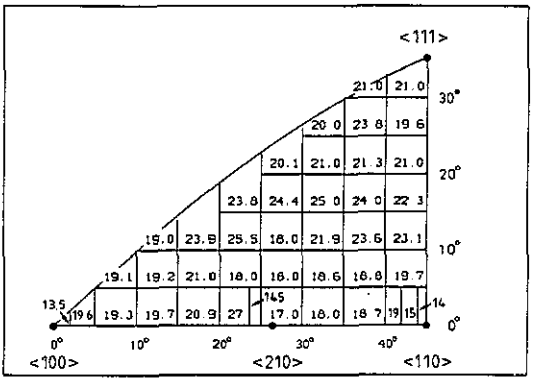

Figure 4. Threshold surface of Ag at 473 K as obtained by varying the E_d values (given in eV) of the 38 elements of the orientation triangle until a good fit to the measured total cross sections was achieved. However, the 500 keV data were not reproduced satisfactorily by this threshold surface. Therefore small areas of low E_d were inserted (cf figure 4). The edge length of the elements corresponds to 5°.

at ⟨100⟩ and ⟨110⟩. The minimum close to ⟨210⟩ might well be localized at ±(2–3)° apart from the position given in figure 4.

The theoretical cross sections calculated with the threshold surface of figure 4 are shown in figure 5 as open diamonds.

The changes introduced to the original threshold surface resulted in a slight worsening of the reproduction of the 600 keV data but they did not affect σ at 700–1000 keV. The latter observation is due to the fact that the maximal transferred energy ΔE^{max} at 700 keV is 23.9 eV and therefore most of the E_d elements of the threshold surface shown in figure 4 (not only the changed ones) contribute to σ (700 keV).

In order to judge the degree of agreement between experimental and theoretical cross sections at the five electron energies used one must keep in mind that one set of E_d elements has to reproduce cross sections ranging from 0.1–55 b. As previously mentioned, this method yields very reliable data on the minima of the threshold surface concerning both the E_d value (typical error ±0.5 eV) and the positions of the minima, whereas the fit is more insensitive to changes in high E_d values. Therefore

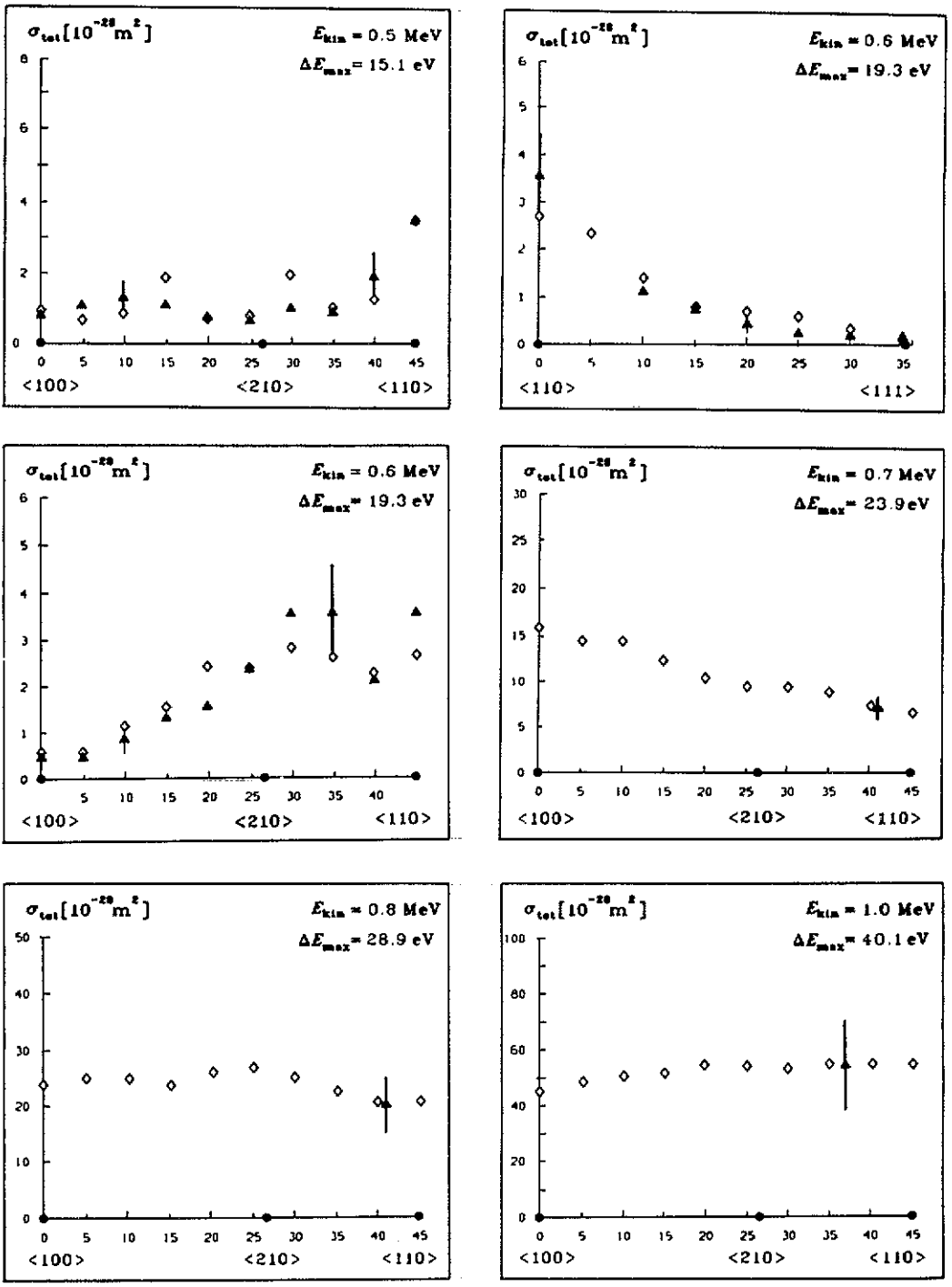

Figure 5. Total cross section for atom displacement in Ag as a function of the direction of irradiation at electron energies of 0.5, 0.6, 0.7, 0.8 and 1 MeV. The full triangles are experimentally determined cross sections. The diamonds are calculated values using the threshold surface of figure 4.

only minima of the threshold surface will be discussed.

The specific features of the threshold surface are three local minima (E_d = 13.5–15 eV) at ⟨100⟩, ⟨110⟩ and ⟨210⟩. All three minima are surrounded by areas at a higher E_d level (17–18 eV at ⟨210⟩, 18–19 eV at ⟨110⟩ and 19–20 eV at ⟨100⟩). Atom displacement along ⟨111⟩ requires average transferred energies of 20.5 eV which is higher than those previously mentioned. However, the ratio $E_d^{\langle 111\rangle}/E_d^{\langle 110\rangle}$ is surprisingly small compared with results obtained on Au (Hohenstein *et al* 1989).

5. Discussion

There are only a few publications concerning the determination of E_d in Ag. Lucasson and Walker (1962) measured the residual electrical resistance after electron irradiation at approximately 20 K in a polycrystalline Ag foil. The electron energies used were 0.83–1.32 MeV. A threshold energy of 28 eV corresponding to an electron kinetic energy of 780 keV was deduced. Considering that damage rate curves usually show a decreasing slope if the electron energy comes close to the threshold energy—be it by subthreshold damage or by local minima in the threshold surface—E_d values of 24 eV (E_{kin} = 700 keV) are compatible with the measured curve. Lucasson (1975) gives an E_d value of 25 eV.

Mitchell *et al* (1975) used the nucleation method to determine E_d by HVEM. At room temperature they irradiated a single crystal along ⟨110⟩ and found the threshold energy to be 23 eV (E_{kin} = 675 keV).

Using the resistivity method, Roberts *et al* (1966) found E_d at 7 and 75 K to be less than or equal to 24 eV. Since no change in E_d below and above stage I recovery was found, it was concluded that the threshold for the production of well separated defect pairs is similar if not lower than that for close pairs. This would be an indication for the importance of RCSs in the production of Frenkel pairs. However, similar results (i.e. no change of E_d in this low-temperature regime) were obtained for different metals by Urban *et al* (1982). Only at higher temperatures were decreases in E_d distinctly seen.

The average E_d values of the present investigation at 473 K are lower by a factor of about 0.75 compared with the low-temperature data of Lucasson and Walker (1962) and Roberts *et al* (1966). Thus the temperature dependence of E_d appears to be less pronounced in Ag than in Au and Cu where this ratio was found to be 0.6.

As previously mentioned Hohenstein *et al* (1989) found a correlation between the α ratio and details of the threshold surface. The metal exhibiting the highest α, namely Au, shows a minimum of E_d at ⟨100⟩ which is distinctly lower than $E_d^{\langle 110\rangle}$. Metals with low α such as Al and Ni possess minima of E_d at ⟨110⟩. $E_d^{\langle 100\rangle}$ is much higher in these metals. Cu, which represents a metal of intermediate α, has minima of E_d both in the ⟨100⟩ and ⟨110⟩ directions.

The underlying cause of the correlation between α value and threshold anisotropy is the mechanism of propagation of the RCS along close-packed directions. At low α collision sequences propagate preferentially along the most close-packed crystallographic direction. In FCC metals this is the ⟨110⟩-direction. RCSs along other close-packed directions are very likely to defocus which results in a short range of the RCS.

At high α values the energy dissipation originating from the interaction of the atoms in a collision sequence with the surrounding 'window atoms' becomes important. These 'window atoms' are most easily displaced by a ⟨100⟩ RCS. Furthermore, assisted

focusing is more likely to occur in this direction than along ⟨110⟩. Consequently metals with large α show minima of E_d close to ⟨100⟩.

As discussed in section 4, the threshold surface of Ag exhibits localized minima at ⟨100⟩, ⟨110⟩ and ⟨210⟩, each of them surrounded by an area of slightly higher threshold energy. The magnitude of E_d at these minima is comparable. Remembering the correlation between E_d and α this means *that the threshold surface of Ag is much more similar to that of Cu than that of Au.* This result shows the singular anisotropy of Au among the FCC metals. It is known that the low-temperature annealing behaviour of Au is unique among the FCC metals (no free migration of interstitial atoms below stage III has been observed). We strongly suggest that these phenomena have their common origin in the high α value of Au.

One could argue at this point that α_{Ag} is very close to α_{Au} and therefore both metals should respond in a similar way to electron irradiation. However, at large α values the influence of the atomic structure of the colliding atoms on the collision process has to be taken into account. The different electron structure of Ag and Au is most readily seen in the different colours of Ag and Au which stems from the energy difference between outer d electrons and the conduction band.

From the theoretical point of view it is known from first-principle calculations that in order to calculate the cohesive energy and the bulk moduli or to predict the correct crystal structure in high-Z materials such as Au, relativistic effects have to be considered. They tend to lower the energy of the s-like bands relative to the d-like bands leading to an increased hybridization of s- and d-electrons and thus to a stronger binding (Takeuchi *et al* 1989a, 1989b; Elsässer *et al* 1991). The equivalence of the lattice parameters of Ag and Au, in spite of the additional electrons in Au, has its origin in this relativistic effect too. This leads to a higher electron density between the atoms in Au and thus, in the case of colliding atoms, to a stronger interaction. As a consequence, the window-opening mechanism previously referred to is more relevant in Au than in Ag. In other words, the relativistic effect causes the *effective* ionic radius in Au and hence the *effective* α to exceed that of Ag to such an extent that the response to radiation damage is markedly different in these metals.

References

Elsässer C, Takeuchi N, Ho K M, Chan C T, Braun P and Fähnle M 1991 *J. Phys.: Condens. Matter* 2 4371

Hohenstein M, Seeger A and Sigle W 1989 *J. Nucl. Mater.* 169 3

Lucasson P G 1975 *Proc. Int. Conf. on the Fundamental Aspects of Radiation Damage in Metals (Gatlinburg, TN, 1975)* USERDA Conf.-751006-P1,42

Lucasson P G and Walker R M 1962 *Phys. Rev.* 127 485

Lyles R L, Rothman S J and Jäger W 1978 *Metallography* 11 361

Mitchell M G, Das G and Kenik E A 1975 *Proc. Int. Conf. on the Fundamental Aspects of Radiation Damage in Metals (Gatlinburg, TN, 1975)* USERDA Conf.-751006-P1,73

Roberts C G, Rickey W P and Shearin P E 1966 *J. Appl. Phys.* 37 4517

Takeuchi N, Chan C T and Ho K M 1989a *Phys. Rev.* B 40 1565

—— 1989b *Phys. Rev. Lett.* 63 1273

Urban K, Saile B, Yoshida N and Zag W 1982 *Proc. 5th Yamada Conf. on Point Defects and Defect Interactions in Metals* ed J-I Takamura, M Doyama and M Kiritani (Kyoto: University of Tokyo Press) p 783

Urban K and Yoshida N, 1981 *Phil. Mag.* A 44 1193